Projet de note aux C. R. Acad. Sci. Paris, Série I, p.iii–jjj, YYYY
Analyse numérique/*Numerical Analysis*

Filter-based stabilization of spectral element methods

Paul FISCHER[a], Julia MULLEN[b]

[a] **Mathematics and Computer Science Div., Argonne National Laboratory, Argonne, IL, USA 60439**
[b] **Division of Applied Mathematics, Brown Univ., Providence RI, USA 02912**

(Proposée le 19 Juliet 1999)

Abstract. *We present a simple filtering procedure for stabilizing the spectral element method (SEM) for the unsteady advection-diffusion and Navier-Stokes equations. A number of example applications are presented, along with basic analysis for the advection-diffusion case.*

Stabilisation par filtrage pour la méthode des éléments spectraux

Résumé. Nous présentons une procédure simple de filtrage pour la stabilisation de la méthode des éléments spectraux (SEM) appliquée à des équations de convection-diffusion et de Navier-Stokes. Cette procédure est mise en oeuvre sur un grand nombre d'exemples, et une analyse élémentaire est réalisée sur un cas de convection-diffusion.

1. Introduction

We consider spectral element solution of the incompressible Navier-Stokes equations in $\mathbb{R}^d$,

$$\frac{\partial \mathbf{u}}{\partial t} + \mathbf{u}\cdot\nabla\mathbf{u} \;=\; -\nabla p \;+\; \frac{1}{Re}\nabla^2\mathbf{u} \;\text{ in } \Omega, \quad \nabla\cdot\mathbf{u} \;=\; 0 \;\text{ in } \Omega, \tag{1}$$

with prescribed boundary and initial conditions for the velocity, $\mathbf{u}$. Here, p is the pressure and $Re = \frac{UL}{\nu}$ the Reynolds number based on characteristic velocity and length scales.

A well-known difficulty in numerical treatment of (1) is the enforcement of the divergence-free constraint on $\mathbf{u}$, particularly at high Reynolds numbers. The $\mathbb{P}_N - \mathbb{P}_{N-2}$ spectral element method (SEM) introduced in [9] addresses this problem through the use of compatible velocity and pressure spaces that are free of spurious modes. The method attains exponential convergence in space and second- or third-order accuracy in time. Despite these advantages, we have in the past encountered stability problems that have mandated very fine resolution for applications at moderate to high Reynolds numbers (10^3–10^4). Here, we demonstrate a simple filtering procedure that largely cures the instability and allows one to recover the full advantages of the SEM.

2. Discretization and Filter

The filter is applied at the end of each step of the Navier-Stokes time integration (described in detail in [7]). The temporal discretization is based on the high-order operator-splitting methods developed in [10].The convective term is expressed as a material derivative, which is discretized using a stable second-order BDF scheme, leading to a linear symmetric Stokes problem to be solved implicitly at each step. The subintegration of the convection term permits timestep sizes,

Projet de note proposé à

Δt, corresponding to convective CFL numbers of 2–5, thus significantly reducing the number of (expensive) Stokes solves.

The Stokes discretization is based on the variational form *Find* $(\mathbf{u},p)\in X_N\times Y_N$ *such that*

$$\frac{1}{Re}(\nabla\mathbf{u},\nabla\mathbf{v})_{GL}+\frac{3}{2\Delta t}(\mathbf{u},\mathbf{v})_{GL}-(p,\nabla\cdot\mathbf{v})_G=\ (\mathbf{f},\mathbf{v})_{GL},\quad(\nabla\cdot\mathbf{u},q)_G=\ 0, \tag{2}$$

$\forall\,(\mathbf{v},q)\in X_N\times Y_N$. The inner products $(.,.)_{GL}$ and $(.,.)_G$ refer to the Gauss-Lobatto-Legendre (GL) and Gauss-Legendre (G) quadratures associated with the spaces $X_N:=[Z_N\cap H_0^1(\Omega)]^d$ and $Y_N:=Z_{N-2}$, respectively. Here, $Z_N:=\{v\in L^2(\Omega)|v_{|\Omega^k}\in\mathbb{P}_N(\Omega^k)\}$, where L^2 is the space of square integrable functions on Ω; H_0^1 is the space of functions in L^2 that vanish on the boundary and whose first derivative is also in L^2, and $\mathbb{P}_N(\Omega^k)$ is the space of functions on Ω^k whose image is a tensor-product polynomial of degree $\leq N$ in the reference domain, $\hat{\Omega}:=[-1,1]^d$. For $d=2$, a typical element in X_N is written

$$\mathbf{u}(\mathbf{x}^k(r,s))\big|_{\Omega^k}\ =\ \sum_{i=0}^{N}\sum_{j=0}^{N}\mathbf{u}_{ij}^k h_i^N(r)h_j^N(s)\,, \tag{3}$$

where $\mathbf{u}_{ij}^k$ is the nodal basis coefficient; $h_i^N\in\mathbb{P}_N$ is the Lagrange polynomial based on the GL quadrature points, $\{\xi_j^N\}_{j=0}^N$ (the zeros of $(1-\xi^2)L_N'(\xi)$, where L_N is the Legendre polynomial of degree N); and $\mathbf{x}^k(r,s)$ is the coordinate mapping from $\hat{\Omega}$ to Ω^k. We assume $\Omega=\cup_{k=1}^K\Omega^k$ and that $\bar{\Omega}^k\cap\bar{\Omega}^l$ for $k\neq l$ is either an entire edge, a single vertex, or void. Function continuity ($\mathbf{u}\in H^1$) is enforced by ensuring that nodal values on element boundaries coincide with those on adjacent elements. For Y_N, a tensor-product form similar to (3) is used, save that the interpolants are based on the G points since interelement continuity is not enforced.

Insertion of the SEM basis into (2) yields a discrete Stokes system to be solved at each step:

$$H\,\underline{\tilde{\mathbf{u}}}-D^T\,\underline{p}^n=B\,\underline{\mathbf{f}}^n,\ \ D\,\underline{\tilde{\mathbf{u}}}=0;\quad \underline{\mathbf{u}}^n=F_\alpha\underline{\tilde{\mathbf{u}}},$$

where we have introduced the stabilizing filter, F_α, to be described below. Here, $H=\frac{1}{Re}A+\frac{1}{\Delta t}B$ is the discrete equivalent of the Helmholtz operator, $(\,-\frac{1}{Re}\nabla^2+\frac{1}{\Delta t})$; $-A$ is the discrete Laplacian; B is the mass matrix associated with the velocity mesh; D is the discrete divergence operator, and $\underline{\mathbf{f}}^n$ accounts for the explicit treatment of the nonlinear terms. The filter, F_α, is applied on an element-by-element basis once the velocity-pressure pair $(\underline{\tilde{\mathbf{u}}},\underline{p}^n)$ has been computed.

The filter is constructed as follows. Let i_n be the one-dimensional interpolation operator at the nodes $\{\xi_j^n\}_{j=0}^n$ over $\mathbb{P}_n[-1,1]$. Then in the square, we can define i_n^r (resp. i_n^s) as being the interpolation operator in the r (resp. s) direction. The filter (in the square) is then $F_\alpha=\alpha I_{N-1}+(1-\alpha)Id$, where $I_{N-1}=i_{N-1}^r\circ i_{N-1}^s$ and Id is the identity operator. The interpolation-based procedure ensures that interelement continuity is preserved; and, because the nodal basis points ξ_i^N interlace ξ_i^{N-1}, F_α will tend to dampen high-frequency oscillations. Moreover, spectral convergence is not compromised, because the interpolation error will go to zero exponentially fast as $N\longrightarrow\infty$ for smooth u. This operator is stable both in L^2 and H^1 norms (that are natural norms for this equation) as can be found in [2] (13.27–28). We note that $\alpha=1$ corresponds to a full projection onto $\mathbb{P}_{N-1}$, effectively yielding a sharp cutoff in modal space, whereas $0<\alpha<1$ yields a smoother, preferable decay [3, 6, 8].

3. Applications

We have used the filtering procedure on a number of high Reynolds number applications where the standard $\mathbb{P}_N-\mathbb{P}_{N-2}$ method would not converge (for reasonable values of K and N). These

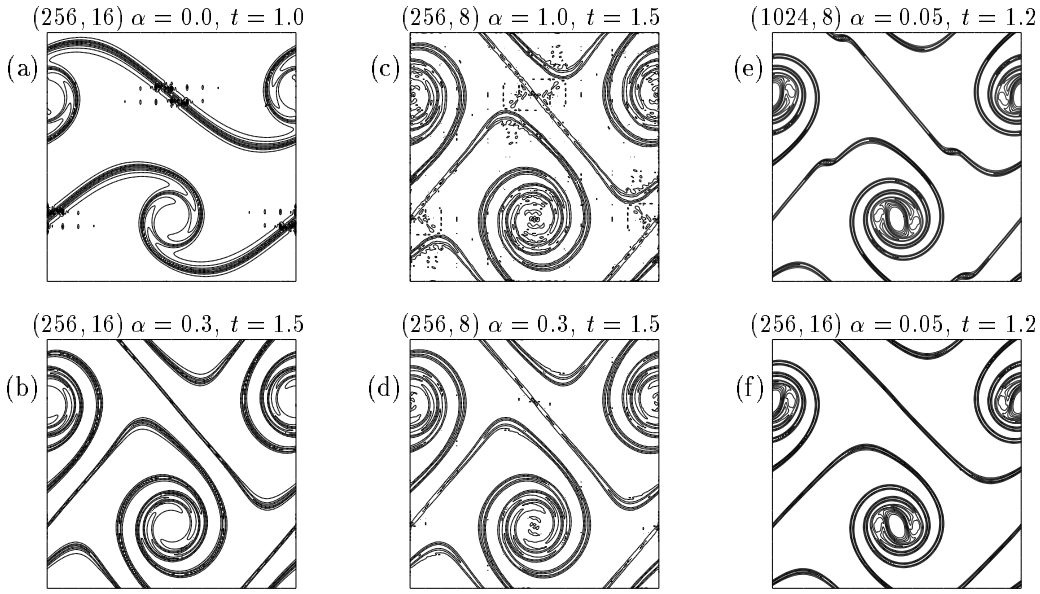

Figure 1: Vorticity for different (K, N) pairings: (a–d) $\rho = 30$, $Re = 10^5$, contours from -70 to 70 by 140/15; (e–f) $\rho = 100$, $Re = 40,000$, contours from -36 to 36 by 72/13. (cf. Fig. 3c in [4]).

have included the regularized driven cavity at $Re = 5000$, transitional channel flow at $Re_h = 8000$, and hairpin vortex formation in a boundary layer at $Re_\delta = 1200$. The examples below demonstrate the benefits of the filter on some well-known test problems.

Example 1. Figure 1 shows results for the shear layer roll-up problem studied in [1, 4]. Doubly-periodic boundary conditions are applied on $\Omega := [0, 1]^2$, with initial conditions

$$u = \tanh(\rho(y - 0.25)) \text{ for } y \leq 0.5, \quad u = \tanh(\rho(0.75 - y)) \text{ for } y > 0.5, \quad v = 0.05 \sin(2\pi x).$$

Each case consists of a 16×16 array of elements, save for (e), which is 32×32. The time step size is $\Delta t = .002$ in all cases, corresponding to CFL numbers in the range of 1 to 5. Without filtering, we are unable to simulate this problem at any reasonable resolution. In (a), we see the results just prior to blow up for the unfiltered case with $N = 16$, corresponding to an $n \times n$ grid with $n = 256$. Unfiltered results for $N = 8$ ($n = 128$) and $N = 32$ ($n = 512$) are similar. Filtering with $\alpha = 0.3$ yields dramatic improvement for $n = 256$ (b) and $n = 128$ (d). Although full projection ($\alpha = 1$) is also stable, it is clear by comparing (c) with (d) that partial filtering ($\alpha < 1$) is preferable. Finally, (e) and (f) correspond to the difficult "thin" shear layer case [4]. The spurious vortices in (e) are eliminated in (f) by increasing the order to $N = 16$ at fixed resolution ($n = 256$). Note that an even number of contours was chosen to avoid the dynamically insignificant zero contour.

Example 2. The spatial and temporal accuracy of the filtered SEM is verified by reconsidering the Orr-Sommerfeld problem studied in [7]. The growth rates of a small-amplitude (10^{-5}) Tollmien-Schlichting wave superimposed on plane Poiseuille channel flow at $Re = 7500$ are compared with the results of linear theory. The errors (see (41) in [7]) at time $t = 60$ given in Table 1 reveal exponential convergence in N for both the filtered and unfiltered cases. It is also clear that $O(\Delta t^2)$ and $O(\Delta t^3)$ convergence is obtained for the filtered case, but that the unfiltered results are unstable for the third-order scheme. In this case, the stability provided by the filter permits the use of higher-order temporal schemes, thereby allowing a larger time step for a given accuracy.

Table 1: Spatial and Temporal Convergence, Orr-Sommerfeld Problem

	$\Delta t = 0.00325$		$N = 17$	2nd-order		3rd-order	
N	$\alpha = 0.0$	$\alpha = 0.2$	Δt	$\alpha = 0.0$	$\alpha = 0.2$	$\alpha = 0.0$	$\alpha = 0.2$
7	0.23641	0.27450	0.20000	0.12621	0.12621	171.370	0.02066
9	0.00173	0.11929	0.10000	0.03465	0.03465	0.00267	0.00268
11	0.00455	0.01114	0.05000	0.00910	0.00911	161.134	0.00040
13	0.00004	0.00074	0.02500	0.00238	0.00238	1.04463	0.00012

4. Analysis and Conclusion

The stabilizing role of the filter is illustrated by considering a time marching approach to solving the advection-diffusion equation, $u_x = \nu u_{xx} + f$, $u(0) = u(1) = 0$, which was studied in the context of bubble-stabilized spectral methods in [5]. Discretization by SEM/CN-AB3 yields

$$H\tilde{\underline{u}} = H_R \underline{u}^n + C(\frac{23}{12}\underline{u}^n - \frac{16}{12}\underline{u}^{n-1} + \frac{5}{12}\underline{u}^{n-2}) + B\underline{f}\,, \quad \underline{u}^{n+1} = F_\alpha \tilde{\underline{u}}\,, \tag{4}$$

where $H = (\frac{\nu}{2}A + \frac{1}{\Delta t}B)$ and $H_R = (-\frac{\nu}{2}A + \frac{1}{\Delta t}B)$ are discrete Helmholtz operators and C is the convection operator. The fixed point of (4) satisfies

$$\left(-\nu A + C + H(F_\alpha^{-1} - I)\right)\underline{u} = B\underline{f}\,. \tag{5}$$

The Δt dependence in (5) can be eliminated by assuming that $1 \simeq \mathrm{CFL} := \Delta t/\Delta x \simeq \Delta t N^2$.

For any Galerkin formulation, C is skew symmetric and therefore singular if the number of variables is odd (the spurious mode being $L_N - L_0$). The eigenvalues of $(F_\alpha^{-1} - I)$ are $\{0, 0, \ldots, 0, \frac{\alpha}{1-\alpha}\}$ (the non-zero eigenmode being $\phi_N(x) := \frac{2N-1}{N(N-1)}(1-x^2)L'_{N-1}(x) = L_N - L_{N-2}$). The stabilizing term, $H(F_\alpha^{-1} - I)$, thus prevents (5) from blowing up as $\nu \longrightarrow 0$ by suppressing the unstable mode. We note that this mode corresponds to a single element in the filter basis suggested in [3]. One can easily suppress more elements in this basis in order to construct smoother filters as suggested, for example, in [3, 6, 8]. However, our early experiences and asymptotic analysis ($\nu \longrightarrow 0$ in (5)) indicate that slight suppression of just the Nth mode is sufficient to stabilize the $\mathbb{P}_N - \mathbb{P}_{N-2}$ method at moderate to high Reynolds numbers.

References

[1] J. B. Bell, P. Collela, and H. M. Glaz, A second-order projection method for the incompressible Navier-Stokes equations, J. Comp. Phys., 85, (1989) 257–283.

[2] C. Bernardi and Y. Maday, Spectral Methods, in Handbook of Numerical Analysis P. G. Ciarlet and J. L. Lions, eds., North-Holland (1999).

[3] J. P. Boyd, Two comments on filtering for Chebyshev and Legendre spectral and spectral element methods, J. Comp. Phys., 143, (1998) 283–288.

[4] D. L. Brown and M. L. Minion, Performance of under-resolved two-dimensional incompressible flow simulations, J. Comp. Phys., 122, (1995) 165–183.

[5] C. Canuto and G. Puppo, Bubble stabilization of spectral Legendre methods for the advection-diffusion equation, Comput. Methods Appl. Mech. Engrg., 118, (1994) 239-263.

[6] W. S. Don and D. Gottlieb, Spectral simulation of supersonic reactive flows, SIAM J. Numer. Anal. 35 (1998) 2370–2384.

[7] P. F. Fischer, An overlapping Schwarz method for spectral element solution of the incompressible Navier-Stokes equations, J. Comp. Phys., 133, (1997) 84–101.

[8] Y. Maday, S. Ould Kaber, and E. Tadmor, Legendre pseudospectral viscosity method for nonlinear conservation laws, SIAM J. Numer. Anal., 30, (1993) 321–342.

[9] Y. Maday, and A. T. Patera, Spectral element methods for the Navier-Stokes equations in State of the Art Surveys in Computational Mechanics, A.K. Noor, ed., ASME, New York, (1989) 71-143.

[10] Y. Maday, A. T. Patera, and E. M. Rønquist, An operator-integration-factor splitting method for time-dependent problems: Application to incompressible fluid flow, J. Sci. Comput., 5(4), (1990) 310-37.